

Dense Video Object Captioning from Disjoint Supervision

Xingyi Zhou* Anurag Arnab* Chen Sun Cordelia Schmid
Google

Abstract. We propose a new task and model for *dense video object captioning* – detecting, tracking and captioning trajectories of objects in a video. This task unifies spatial and temporal localization in video, whilst also requiring fine-grained visual understanding that is best described by natural language. We propose a unified model, and demonstrate how our end-to-end approach is more accurate and temporally coherent than a multi-stage pipeline combining state-of-the-art detection, tracking, and captioning models. Moreover, we propose a training strategy based on a mixture of disjoint tasks, which allows us to leverage diverse, large-scale datasets which supervise different parts of our model. Although each pretraining task only provides weak supervision, they are complementary and, when combined, result in noteworthy zero-shot ability and serve as strong initialization for additional finetuning to further improve accuracy. We carefully design new metrics capturing all components of our task, and show how we can repurpose existing video grounding datasets (*e.g.* VidSTG and VLN) for our new task. We show that our model improves upon a number of strong baselines for this new task. Furthermore, we can apply our model to the task of spatial grounding, outperforming prior state-of-the-art on VidSTG and VLN, without explicitly training for it. Code is available at <https://github.com/google-research/scenic>.

Keywords: vision-and-language · object captioning · tracking · video

1 Introduction

Powered by gigantic datasets and models, *language* is becoming the output modality of the most capable artificial intelligence models [1, 10, 35, 42, 46, 57]. Language unifies different tasks with the same output space [11, 49], is more descriptive than discrete class labels [43, 65], and naturally facilitates zero-shot prediction of novel tasks [10, 48]. Inspired by advances in natural language understanding, the vision community has explored language in a number of tasks including image captioning [13], dense image captioning [34], question answering [3], video captioning [45] and representation learning [48]. However, likely due to the scarcity of large-scale, aligned training data, we are not aware of any existing single vision-language model that unifies both fine-grained spatial- (by detecting objects) and temporal- (by reasoning across time in videos) understanding.

In this paper, we propose a new task and model for *dense video object captioning* (Dense VOC) – the task of generating captions of object trajectories from video (Fig. 1). Dense VOC is therefore a superset of independent tasks

* Equal contribution. {zhouxy, aarnab}@google.com

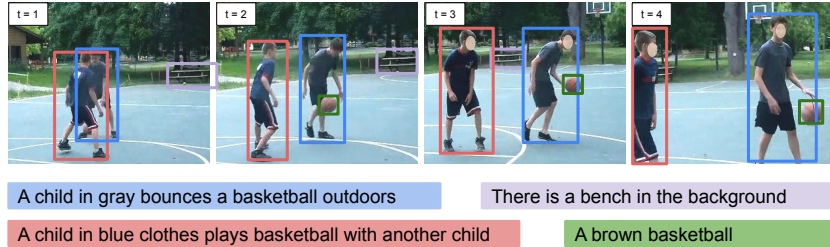


Fig. 1: Overview of the dense video object captioning (Dense VOC) task. Given a video, we predict object trajectories (identities are denoted by colors) and their natural language description. Our task involves object detection, tracking, and captioning. We show a video from the VidSTG [83] validation set.

commonly studied in vision – namely object detection [24, 41], multi-object tracking [17, 19] and captioning [13, 45], as it requires understanding across space, time and language (Fig. 2).

A prominent challenge for training our model is that datasets with captioned trajectories are scarce. To address this, we design our end-to-end model such that it has separate, but interlinked stages for object proposals, tracking and captioning. Thanks to this design choice, we can train our model without any full annotations for the Dense VOC task by using a mixture of *disjoint* tasks and datasets that supervise different parts of our model. For example, we can train our object proposal component using image-level object detection labels from COCO [41], and the captioning component from video-level captioning datasets like SMiT [45]. Our disjoint pretraining tasks are complementary, and in combination supervise our entire model. This enables us to perform our Dense VOC task in a zero-shot manner, and we show that we can achieve noteworthy performance despite not having access to any full, captioned object trajectories during training. Furthermore, this pretraining serves as a powerful initialization for finetuning on the full Dense VOC task, where limited annotations are available.

Another challenge in our task is to produce holistic and consistent captions for objects across frames. Note that a baseline of applying a strong, dense image captioning model per-frame, and then linking objects together is poorly suited to this scenario: the captions at each frame are likely to be different due to subtle appearance changes across frames. This motivates our end-to-end trained model, which includes a novel end-to-end tracking algorithm that efficiently aggregates features of the same object across time, enabling the subsequent captioning module to leverage global video features to produce coherent captions.

To evaluate our model, we develop a new metric that jointly measures performance on captioning, detection and tracking by extending HOTA [44], the most popular metric for multi-object tracking. Although we are the first to our knowledge to study Dense VOC, we can still repurpose existing video grounding datasets for evaluation and domain-specific finetuning. We use VidSTG [83] and VLN [60], originally designed for spatiotemporal sentence grounding: Instead of finding an object tube given a sentence query (grounding), we predict object trajectories directly and use the sentence queries as the ground truth captions.

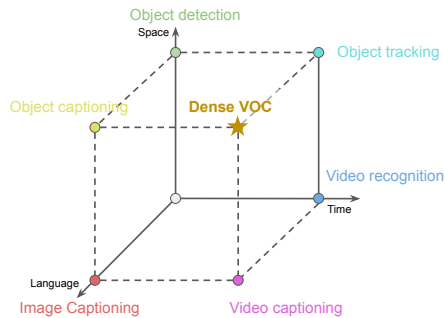


Fig. 2: Overview of Dense VOC. Our problem involves understanding across space, time and language, and thus encompasses other vision tasks, which typically consider one or two of these axes. We also show how these subtasks are complementary, and how pretraining on them enables zero-shot generalization to Dense VOC.

spatial grounding models on both VidSTG and VLN. In summary, we propose the following contributions:

1. We propose the new task of Dense Video Object Captioning. We propose novel evaluation metrics, and repurpose existing grounding datasets for evaluation.
2. We design an end-to-end architecture for our task, with a novel tracking algorithm and feature aggregator that ensures temporally consistent captions. Unlike conventional offline trackers, our tracker is trained end-to-end with the model and produces long-term trajectory features for subsequent captioning.
3. We show our model can be trained without full annotations for the task, with a mixture of disjoint datasets which supervise different parts of our model.
4. We further show how our models generalize to downstream grounding tasks, achieving state-of-the-art results on two datasets, without explicitly being trained on grounding tasks.

2 Related Work

Image captioning [2, 13, 52, 69] describes the content of an image with language. State-of-the-art methods map the input image to output text by using multi-modal models [20, 30, 35, 38, 78, 80] pretrained on large datasets [48, 55]. For example, GIT [61] simply forwards vision tokens from a ViT encoder [22] to an auto-regressive language decoder [21, 59]. Similar ideas apply to **video captioning** [45, 68, 85], by concatenating [61] or pooling [71] features from each frame, before feeding them to the auto-regressive text decoder. Our work builds on existing captioning architectures [61], and extends them to object trajectory captioning using our end-to-end model and weak supervision [34, 41, 45].

Dense object captioning in contrast, detects objects in an image and describes them with text [32, 37, 54, 65]. It was popularized by the Visual Genome [34]

In addition, we show that our generative model trained for Dense VOC can perform grounding by simply selecting the bounding boxes with the maximum likelihood of producing the query sentence.

Experiments show that our end-to-end trained Dense VOC model outperforms baselines consisting of strong, per-task models by a substantial margin, producing more accurate and inherently temporally consistent captions. Moreover, we achieve significant improvements from our disjoint, multi-dataset training. Furthermore, by applying our generative captioning model to the discriminative grounding task, we are able to outperform dedicated

dataset, which contains full annotations for the task. Early work, DenseCap [32] used a one-stage detector [50] followed by an LSTM text decoder [29] on dense feature maps. Most recently, GRiT [65] built upon the state-of-the-art image captioning architecture of GIT [61], and generated object captions, also with a transformer decoder [59], from RoI-pooled [27] image features. Our model advances architectures like GRiT to videos and incorporates end-to-end tracking of object trajectories too. We also note that **dense video captioning** in the literature refers to the task of localizing and captioning multiple events *temporally* in videos [33, 62, 73, 85]. Our task, in contrast, involves tracking and captioning objects in a video, and therefore requires *spatial* localization, which is why we name our task “dense video object captioning”.

Multi-object tracking aims to detect objects and track them with a consistent identity label. The predominant approach is tracking-after-detection [7, 23, 82], *i.e.* first running detectors on each frame and then using a separate tracker to link them. While this works well for existing benchmarks with only a few classes [19, 25, 74], it is more challenging in our case: we need tracks *before* captioning to have a single, consistent textual output for the whole trajectory. Thus, our work follows **end-to-end multi-object tracking** [14, 36, 64, 89]. We adopt a global tracker GTR [89], which casts tracking as pairwise association among all objects within a video. Whilst GTR applies a sliding-window-based identity association algorithm during inference as a post-processing step, we design an efficient algorithm to perform this process end-to-end. This is necessary for our task, since our trajectory features are used by a subsequent captioning module which is trained jointly. We are not aware of prior work which efficiently assigns object identities and corresponding features to tracks, and trains end-to-end through this process. Finally, we note that **video object tracking and segmentation** [15, 16, 75–77] focuses on following a *single* object which is given in the first frame [47, 70]. This is therefore a different setting from our task of detecting, tracking and captioning multiple objects.

Video object grounding [60, 83] finds a spatio-temporal tube given a video and query sentence as inputs. Existing, discriminative methods [31, 56, 72, 83] co-embed visual and text inputs, and use the sentence feature to find the corresponding object. In contrast, we use our generative language model for this task by selecting the object with the highest likelihood of producing the query. To our knowledge, we are the first work to explore the alternate paradigm of generative models for this task. Finally, we note that these tasks are also related to video-referring segmentation [6, 66, 79] which grounds textual queries to segmentation masks. Segmentation, however, is not the focus of our work.

3 Method

As shown in Fig. 3, our end-to-end trainable model consists of interlinked heads for object proposal, tracking and captioning the resulting trajectories. Before introducing our novel components, we review prior techniques for captioning and dense object captioning in images [61, 65] which our model is built on.

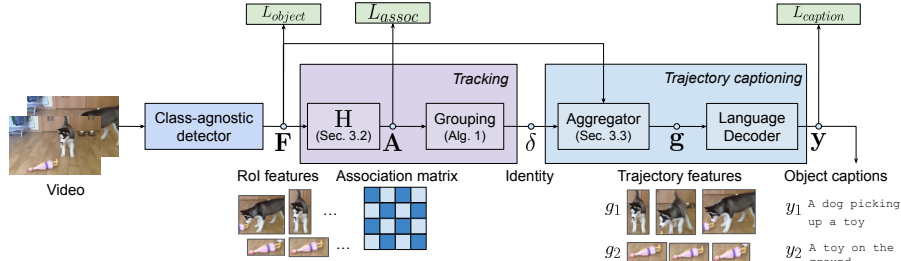


Fig. 3: Overview of our model. Our end-to-end model has three modules: First it produces object proposals per-frame using a class-agnostic detector (left, trained with detection loss, L_{object}). These object proposals are then passed to an end-to-end tracking module that groups objects into trajectories (middle, trained with association loss, L_{assoc}). The identities produced by the tracking module are used to aggregate features which are then fed to a language decoder to produce the final caption (right, trained with caption loss $L_{caption}$). Our full model can be trained end-to-end with Dense VOC supervision when available, or be trained with partial supervision on different and disjoint datasets to provide zero-shot capabilities, and initialization for finetuning.

3.1 Background

Image captioning maps an input image, $\mathbf{I} \in \mathbb{R}^{H \times W \times 3}$, to a caption $c = (y_1, y_2, \dots, y_{n_t})$ which is a sequence of up to n_t text tokens from a given vocabulary. The minimal set of components is an image encoder, followed by a text decoder [59]. The encoder maps the input image \mathbf{I} , to a feature representation $\mathbf{f} \in \mathbb{R}^{n_v \times d}$ consisting of n_v tokens with dimensionality d . The subsequent text decoder is auto-regressive [26, 59] – it predicts the next text token, y_i , as a function of both the image features, \mathbf{f} , and previously generated text tokens, $\mathbf{y}_{0:i-1}$, denoted by $y_i = \text{Decode}(\mathbf{f}, \mathbf{y}_{0:i-1})$. Note that the first step of decoding begins with $y_0 = \text{BOS}$, a special beginning-of-sentence token, and the caption ends when the end-of-sentence token, EOS , is output by the model. This simple image captioning model has been demonstrated to be effective and scalable by GIT [61], achieving state-of-the-art results across a number of captioning datasets.

GRiT [65] extends the approach further to dense object captioning of images: Here, the authors use an object proposal network [88] to produce a set of K class-agnostic bounding boxes, b_1, b_2, \dots, b_K . Features corresponding to each of these objects are obtained using RoIAlign [27], resulting in a localized feature, $f_k \in \mathbb{R}^{r \times r \times d}$ where $r = 7$ is the output resolution of RoIAlign. Each of these grid features is flattened into $f_k \in \mathbb{R}^{r^2 \times d}$ and decoded independently by the text decoder, as done in GIT [61]. Therefore, the loss used to train a GRiT model consists of $L = L_{object} + L_{caption}$ where $L_{caption}$ is a cross-entropy loss over all text tokens in the vocabulary, and L_{object} consists of bounding box regression and objectness terms, as standard in object detection literature [40, 51, 88].

We now describe how we extend object captioning to videos by tracking object proposals over time (Sec. 3.2) and aggregating trajectory features and captioning them (Sec. 3.3) in an end-to-end fashion. Section 3.4 explains how we train our model, whilst Sec. 3.5 describes how we apply our model directly to video object grounding tasks.

Algorithm 1: Identity assignment from association matrix. This greedy algorithm can be implemented efficiently on accelerators, allowing us to train end-to-end with it.

Input : Association Matrix $\mathbf{A} \in \mathbb{R}^{TK \times TK}$, where T denotes the number of frames, and K the number of objects per frame.

Hyper parameters: Association score threshold θ

Output : Identities for each object $\delta \in \mathbb{N}^{TK}$

$M \leftarrow T \times K$ // Number of total objects.

$A \leftarrow \text{preprocess}(A)$ // Preprocess A to ensure object pairs in the same frame have a score of 0.

$\hat{A} \leftarrow (A \geq \theta).astype(\text{bool})$ // Binary matrix for possible merges.

$\delta \leftarrow \text{zeros}(M)$ // Initialize output identities, shape $(M,)$

$\text{id_count} \leftarrow 0$ // Initialize ID count.

while $\hat{A}.any() > 0$ **do**

$\text{track_len} \leftarrow \hat{A}.sum(\text{axis}=1)$ // Compute the number of objects in each merge.

$i \leftarrow \text{track_len}.argmax()$ // Find the longest track to merge.

$\text{id_count} \leftarrow \text{id_count} + 1$ // Create a new identity.

$\delta \leftarrow \delta + \text{id_count} * \hat{A}_i$ // Assign the current track a new ID using \hat{A}_i as the binary mask.

$\hat{A} \leftarrow \hat{A} - \hat{A}_i | \hat{A}_i$ // Remove merged indices. “|” is logical or.

end

return δ

3.2 End-to-end tracking

As shown in Fig. 3 (left), we first produce object proposals separately for each frame. Tracking then aims to assign each object in each frame a unique trajectory identity $\delta \in \mathbb{N}$. We define $\mathbf{f}_k^t \in \mathbb{R}^{r^2 \times d}$ as the ROI feature of object proposal k in frame t , $\mathbf{F} = [\mathbf{f}_k^t]_{t=1, k=1}^{T, K_t}$ as the concatenation of all object features in the video. Let $M = |\mathbf{F}| = \sum_{t=1}^T K_t$ as the total number of objects in all frames, where K_t is the number of object proposals at the t^{th} frame. Thus, we have $\mathbf{F} \in \mathbb{R}^{M \times r^2 \times d}$.

From these object features, \mathbf{F} , we predict a global association matrix, $\mathbf{A} \in \mathbb{R}^{M \times M}$, where $\mathbf{A}_{ij} = 1$ if the objects denoted by the i^{th} row and j^{th} column are from the same trajectory (Fig. 3 middle). Otherwise, $\mathbf{A}_{ij} = 0$ meaning that these objects are from different trajectories, or at least one of them is background.

We use a transformer module, H, with two self-attention layers, similar to GTR [89], to predict the association matrix $\mathbf{A} = \sigma(\text{H}(\mathbf{F}))$, where σ is the sigmoid activation. Given the object trajectory annotations, we construct the ground truth association matrix $\bar{\mathbf{A}}$ for \mathbf{A} , where $\bar{\mathbf{A}}_{ij} = 1$ if and only if row i and column j of \mathbf{A} are matched to the same ground truth trajectory using an Intersection over Union (IoU) criteria of 0.5. The training loss L_{assoc} for this module is then a binary cross entropy between \mathbf{A} and $\bar{\mathbf{A}}$, $L_{assoc} = \frac{1}{M} \sum_{ij} \text{BCE}(A_{ij}, \bar{A}_{ij})$.

After constructing our association matrix, \mathbf{A} , we need to aggregate object-level features according to identities $\delta = [\delta_k^t]_{t=1, k=1}^{T, K_t}$, to generate trajectory-level captions for the next captioning stage. Here, δ_k^t denotes the identity of the k -th object proposal in the t -th frame. We design a greedy grouping algorithm (Alg. 1) operating on \mathbf{A} to obtain δ . Concretely, we greedily extract the longest trajectory from untracked objects, until there are no possible associations left

(indicated by the association score being above a threshold θ). This guarantees that each trajectory has at most one object in each frame. This algorithm can be implemented efficiently on accelerators, allowing us to backpropagate through it.

As aforementioned, prior trackers [82, 86, 87] do not explicitly perform identity assignment within the model, but rather as a post-processing step since tracking is the final output for such methods. Our work efficiently assigns object identities to tracks in an end-to-end trainable network, which enables us to perform joint trajectory-level captioning training as described next.

3.3 Trajectory captioning

Our end-to-end tracking module produces object features, \mathbf{f}_k (we omit the frame index t below for clearer notation), paired with their identities, δ_k , which denote their correspondence over time. We now describe two methods for aggregating features along this trajectory in order to caption it.

Soft aggregation. A straightforward way to leverage object features over time is to compute a weighted sum to combine them into a single, global trajectory feature. We observe that the association matrix, \mathbf{A} (Sec. 3.2), already serves as a summation weight. Specifically, we set $\mathbf{G} = \frac{\mathbf{A}}{\|\mathbf{A}\|} \cdot \mathbf{F}$, where \cdot denotes matrix multiplication, and $\|\cdot\|$ normalizes \mathbf{A} by rows. Each row of \mathbf{G} , $\mathbf{g}_k \in \mathbb{R}^{r^2 \times d}$, therefore denotes an aggregated feature over its trajectory for object k .

Hard aggregation. An alternative to weighted temporal averaging is to concatenate and construct new trajectory features. Let $\mathbf{f}_\tau = \{\mathbf{f}_{k'}\}_{\delta_{k'}=\tau}$ be the set of all object features with identity τ . We note \mathbf{f}_τ can be as long as the entire video, and thus it may be expensive to directly use \mathbf{f}_τ . Therefore, we uniformly sample a subset of object features from the trajectory, denoted as $\mathbf{g}_\tau = \text{UniformSample}(\mathbf{f}_\tau, m)$, where $\mathbf{g}_\tau \in \mathbb{R}^{mr^2 \times d}$, inspired by [61]. m is the number of sampled frames, and we set $m = 6$ following ablations in the supplement.

The trajectory-aggregated features for each object, \mathbf{g}_k , are then autoregressively decoded into output captions for each object, \mathbf{y}_k . This follows Sec. 3.1, where $y_{k,i} = \text{Decode}(\mathbf{g}_k, \mathbf{y}_{k,0:i-1})$. Note that the language decoder has the same parameters as in single-frame object captioning, but processes more input tokens. Therefore, we train it in the same manner with a softmax cross-entropy loss over the vocabulary of text tokens, denoted by $L_{caption}$.

3.4 Pretraining with disjoint subtasks

As shown in Fig. 3, our model is trained with the loss function, $L = L_{object} + L_{assoc} + L_{caption}$. When we have full Dense VOC annotations, which supervise each component of our model we can train our entire model end-to-end.

However, to leverage more weakly-labeled data, we can also decompose Dense VOC into subtasks, and use each subtask to supervise the relevant part of our model using the available annotations as shown in Tab. 1. This approach also enables us to perform our final task in a zero-shot manner (*i.e.* without training on any full Dense VOC annotations).

Dataset	Annotation type	Train size	L_{object}	L_{assoc}	$L_{caption}$
COCO [41]	Image detection	118K	✓		
VG [34]	Image object captioning	70K	✓		✓
SMiT [45]	Video captioning	480K			✓
Aug-COCO [41]	Video object tracking	118K	✓	✓	

Table 1: Datasets for disjoint pretraining. We supervise different losses based on available annotations from each dataset.

Object detection. Using detection datasets for images, we can train the object proposal generator with L_{object} . We use COCO [41] as it is the most popular dataset for this task.

Dense captioning in images. Dense object captioning datasets of images allow us to train both the object proposal generator and the text decoder, by supervising L_{object} and $L_{caption}$. Here, we use Visual Genome [34], the largest dataset for this task.

Global video captioning. Video captioning datasets help us to reduce the domain gap to our final task by also training on video. In particular, we use Spoken Moments in Time (SMiT) [45] which is the largest dataset for this task and contains narrations for short clips (roughly 3 seconds). As there are no object annotations, but only video-level captions, we construct an object proposal from the entire frame and caption that with our text decoder, applying $L_{caption}$. This approach is inspired by prior work on weakly-supervised object detection [4, 8, 86].

Tracking. Training the tracking module of our network (Sec. 3.2) requires annotations that associate detections of an object identity throughout the video. We found that existing tracking datasets either have too limited vocabularies for general objects (MOT [19], KITTI [25], YouTube VIS [74]), or are too small (TAO [17] and UVO [63] label 600 and 5 000 videos respectively). As a result, following existing work [82, 87, 89], we instead augment image datasets into tracking ones by applying two different data augmentations to the same image, and then linearly interpolating the frames in between to form a pseudo-video. In particular, we augment COCO (referred to as Aug-COCO [87]). This enables us to apply L_{assoc} and L_{object} when training our model.

3.5 Application to video object grounding

The task of video object grounding [60, 83] consists of two inputs: a video, \mathbf{V} , and a sentence query, \bar{c} . The output is a sequence of bounding boxes, $[b^s, b^{s+1}, \dots, b^e]$, corresponding to the sentence query, where s and e are the indices of the start and end frames respectively.

Our model, however, generates captions, c , at the output, rather than requiring it as an input. To apply our model to grounding, we follow an analogous approach to prior works that performed closed-set image classification with captioning models [1, 12]: we evaluate the likelihood (i.e., exponential negative cross-entropy loss) of the sentence query, \bar{c} , for each of the object trajectories produced by our model. In practice, we find that instead of just taking the object trajectory with the highest sentence-likelihood, we achieve higher accuracy by weighting the

likelihood by the detection score, s_k , from our object proposal module. Thus, given bounding boxes, trajectory features and detection scores, $\{(b_k^t, s_k^t, \mathbf{g}_k)\}_{t=1, k=1}^{T, K_t}$, we choose the bounding boxes with the highest weighted likelihood:

$$\begin{aligned} k^* &= \arg \max_k (s_k^t \cdot \exp(-L_{caption}(\text{Decode}(\mathbf{f}_k^t), \bar{c}))), \\ b^t &= b_{k^*}^t. \end{aligned} \tag{1}$$

4 Experimental Evaluation

As we are proposing a new task, there is no dedicated dataset or evaluation metric for dense video object captioning. Fortunately, existing video grounding [60, 83] datasets have annotations for object trajectories and their captions, allowing us to repurpose them for Dense VOC, as defined next.

4.1 Datasets

VidSTG [83] was originally created for spatio-temporal sentence grounding, but can be used for Dense VOC: Each video annotates multiple textual queries and their corresponding spatio-temporal tubes. By aggregating these across all videos, we obtain the paired trajectory-caption annotations that we need for training and evaluating our model.

VidSTG has exhaustive trajectory (*i.e.* bounding box and tracking) annotations for all objects [53], but not all objects are used in grounding, and thus not all objects have captions. We account for this fact in both training and testing. Specifically, we do not compute $L_{caption}$ on objects without caption annotations, and also exclude them during evaluation (see Sec. 4.2). In particular, when a prediction is matched to a ground truth without caption annotations, we do not evaluate its captioning metrics, but still evaluate detection metrics. The dataset contains 5 436 training videos and 602 validation videos, with each video being at most 200 frames long. We use the declarative annotations from the dataset containing 19 000 captioned trajectories for training and testing respectively.

Video Localized Narratives (VLN) [60] augments existing datasets by narrating the “main actors” in a video. We therefore use these narrations as our target captions. We use the subset from the UVO dataset [63] as UVO has exhaustive detection and tracking annotations for all objects. Like VidSTG, the captions are not exhaustive for all objects, so we exclude objects without captions in both training and evaluating the captioning module. Each video has bounding box annotations for 3 sparsely sampled frames, and thus we train and evaluate on these frames. The dataset contains a total of 5 136 training and 2 451 validation videos, and 5 588 training and 3 071 validation captioned trajectories.

4.2 Evaluation metrics

Captioned-HOTA (CHOTA). Our primary metric, CHOTA, builds on Higher Order Tracking Accuracy (HOTA) [44] – which is now the most popular metric in multi-object tracking – by adding a captioning term. HOTA decomposes

tracking into two subproblems: detection and association, with the final score being the geometric mean of detection accuracy (DetA) and Association Accuracy (AssA): $\text{HOTA} = \sqrt{\text{DetA} \cdot \text{AssA}}$. Here, $\text{DetA} = \frac{|TP|}{|TP|+|FP|+|FN|}$, and AssA averages the ‘‘Association IoU’’ [44] over true-positive predictions, as $\text{AssA} = \frac{1}{|TP|}(\sum_{(x,y) \in TP} \text{Ass-IoU}(x, y))$, where (x, y) are the matched prediction-ground truth box pairs in each frame. Note that HOTA computes the DetA and AssA for each detection in each frame, rather than for each trajectory, as the overall trajectory performance is implicitly measured by the association of detections over time [44]. Moreover, this approach considers all possible trajectory matches that can be made simultaneously (Sec. 7 of [44]).

Our task consists of captioning, detection and association. Therefore, we also define an additional ‘‘Captioning Accuracy’’ (CapA) term as:

$$\text{CapA} = \frac{1}{3|TP'|} \sum_{(x,y) \in TP'} (\text{METEOR}(x, y) + \text{CIDEr}(x, y) + \text{SPICE}(x, y)) \quad (2)$$

which uses three popular image-captioning metrics [13], and TP' are the true-positive detection pairs that have caption annotations (as discussed in Sec. 4.1.1). Note that for compatibility with HOTA, we follow DetA and AssA and compute CapA separately per-object on each frame. The final metric is then $\text{CHOTA} = \sqrt[3]{\text{DetA} \cdot \text{AssA} \cdot \text{CapA}}$, effectively adding a captioning term to the HOTA metric. Further details are in the supplement.

Frame mAP-METEOR (AP_M). We additionally reuse the evaluation metric for dense object captioning in images from Visual Genome [34]. Note that we avoid the captioning threshold for objects without captioning annotations, as detailed in the supplement. As the original metric was developed for images, it is computed separately on each frame.

4.3 Implementation details

We implement our model in JAX [9] using the scenic library [18]. We use GRiT [65] as our baseline. GRiT uses a ViTDet-Base [22, 39] backbone (initialized with CLIP pretrained parameters [48]), a CenterNet [88] object proposal network and RoI Head, and a randomly-initialized text decoder.

We first train our model for general Dense VOC on large-scale disjoint datasets (Sec. 3.4). During disjoint pretraining, we sample batches from different datasets with an even ratio, (1: 1: 1: 1), thus avoiding additional hyperparameters. For video datasets, we sample 8 frames for a video and use a local batch size of 1. For image datasets, we use a local batch size of 8. We train our model on 32 TPUs, which means we have an effective batch size of 256 images or 32 videos.

We then evaluate the models on the two fully-annotated datasets (Sec. 4.1.1) in both zero-shot and full-finetuning setups. For VidSTG, we sample 16 frames during training, and then run on all 200 frames during testing. For VLN, we use all 3 annotated frames in both training and evaluation. In both cases, we use an input size of 384×384 . During inference, we threshold the outputs of our object proposal module with a score of 0.5, and only track the remaining

#		CHOTA	DetA	AssA	CapA	Consistent captions
1	Per-frame cap. w. IOU tracker	49.9	64.4	52.2	37.1	✗
2	Per-frame cap. w. FairMOT [82]	51.2	63.4	57.2	37.0	✗
3	Per-frame cap. w. ByteTrack [81]	52.3	64.2	60.2	37.1	✗
4	Middle-frame cap. w. ByteTrack [81]	50.7	64.2	60.2	33.8	✓
5	Ours, soft aggregation	54.6	64.4	65.9	38.4	✓
6	Ours, hard aggregation	54.9	64.2	65.9	39.1	✓

Table 2: Comparison of our end-to-end model to per-task baselines on VidSTG validation. Our models are based on #2 of Tab. 4. The image dense captioning models used in the baselines (rows #1-#4), are trained on the same datasets, and run off-the-shelf trackers as a post-processing step. Our end-to-end approach improves across all metrics, and additionally produces temporally consistent captions.

objects. We include exhaustive implementation details and hyperparameters in the supplement and the code.

4.4 Analysis of end-to-end tracking

We first study the benefits of our end-to-end model, and the importance of captioning-after-tracking, in Tab. 2. We do this by comparing to multiple, strong baseline models running in sequence. Concretely, we use the state-of-the-art image-dense object captioning model [65] followed by tracking as a post-processing step. We use trackers ranging from a simple IoU-based tracker [67] to more recent, sophisticated methods like FairMOT [82], and ByteTrack [81].

As the baseline predicts captions independently on each frame, the caption is not consistent over the entire trajectory. Therefore, we consider an additional baseline where we only use the caption from the middle frame of the trajectory. Finally, note that as our baseline captioner is pretrained on Visual Genome, and then finetuned on individual frames of VidSTG, it has been trained on identical data to our model, allowing us to make fair comparisons.

As shown in Tab. 2, per-frame captioners followed by offline trackers produce temporally inconsistent captions (#1-#3). Naively selecting the caption from the middle frame as the trajectory-level caption produces temporally consistent captions, but comes at the cost of captioning accuracy, as a single frame may not be representative of the entire event (#4). Both variants of our model (#5 and #6) improve tracking quality substantially, as shown by their large improvement on AssA, demonstrating the benefits of end-to-end training and incorporating temporal information. Our model improves on CapA too, showing that improved object trajectories provide better features for subsequent captioning. Finally, we note that as expected, the quality of the initial detections at each frame, measured by DetA, does not really change between the baselines and our method. This does, however, show that training our model jointly with multiple loss functions does not compromise performance on individual tasks.

Overall, our end-to-end model (#6) improves the CHOTA by 2.6 points over the best baseline (#3), due to our improvements in AssA and CapA. As hard aggregation performs slightly better, we use it in our following experiments.

#	COCO	VG	SMiT	Aug-COCO	VidSTG					VLN				
					CHOTA	DetA	AssA	CapA	AP _M	CHOTA	DetA	AssA	CapA	AP _M
1	✓				-	48.9	-	-	-	-	27.8	-	-	-
2		✓			-	17.8	-	7.8	17.1	-	12.1	-	7.4	9.9
3			✓		-	-	-	-	-	-	-	-	-	-
4		✓	✓		-	19.1	-	8.5	18.2	-	14.3	-	8.5	12.7
5	✓	✓			-	49.9	-	8.1	37.4	-	28.0	-	7.8	19.7
6	✓		✓		-	50.4	-	4.9	36.7	-	28.7	-	7.5	18.1
7	✓	✓	✓		-	51.3	-	9.1	38.2	-	29.9	-	9.0	19.0
8	✓	✓	✓	✓	31.1	51.4	59.6	9.8	39.5	29.2	29.1	88.0	9.7	20.1

Table 3: Zero-shot evaluation of our disjoint trained models with varying datasets. We show results on VidSTG [83] (center) and VLN [60] (right) without finetuning on them. For models without tracking supervision (#1–7), we cannot report their association accuracy (AssA). Our full model (#8) gains full Dense VOC ability from disjoint training, and shows good performance on all metrics. Notably, CapA is improved given tracking supervision. Detailed captioning metrics are in the supplement.

4.5 Analysis of disjoint training

Zero-shot evaluation. We first pretrain on multiple disjoint datasets (Sec. 3.4), and evaluate zero-shot on our target datasets, VidSTG and VLN, without training on them in Tab. 3. Zero-shot evaluation is simple to perform for models that directly generate text compared to classification, thanks to their open vocabulary. There are, however, significant domain gaps in the object classes, captioning style, and video durations between our training and evaluation datasets.

As mentioned in Tab. 1 and Fig. 3, each dataset supervises different parts of our model. For example, a model that is only trained on COCO (#1 in Tab. 3), is only trained with L_{object} , meaning that it only produces object proposals which we can evaluate with the Detection Accuracy component of our CHOTA metric. Visual Genome (VG) can supervise both the object proposal and captioning heads of our model. However, there is a large domain gap between the captions in VG and our target datasets, since the captions in VG are for single images and focus on very different vocabularies. Furthermore, VG tends to annotate bounding boxes around object parts rather than entire objects. Consequently, our zero-shot DetA is low when training only on VG (#2). Note that we cannot evaluate a model trained only on SMiT, as it does not produce bounding boxes.

We observe in Tab. 3 that the different datasets have complementary properties: Adding COCO improves detection accuracy (#2 to #5, #4 to #7), and adding SMiT improves the captioning accuracy (#2 to #4, #5 to #7) even though SMiT only captions at a video-level. Note that to mitigate the differences in the type of bounding boxes annotated by VG, we ignore L_{object} on it and only compute $L_{caption}$, when using it in conjunction with COCO. Finally, training with Aug-COCO allows us to also supervise L_{assoc} and thus the tracking module of our model. A model trained on all the datasets (#8) can therefore perform the full Dense VOC task, and shows good performance on all individual metrics compared to models trained on fewer datasets. Notably, we observe our final model with tracking improves captioning ability (CapA) without adding captioning training data. Again, similar to Tab. 2, the improvements are likely to result from our ability to leverage temporal information from tracking.

#COCO VG SMiT Aug-COCO	VidSTG					VLN				
	CHOTA	DetA	AssA	CapA	AP _M	CHOTA	DetA	AssA	CapA	AP _M
0	47.8	54.6	57.8	34.5	54.1	29.7	35.3	85.4	8.7	35.1
1 ✓	52.3	64.9	63.0	34.9	69.1	31.8	43.9	88.7	8.2	36.3
2 ✓	54.9	64.2	65.9	39.1	68.7	40.6	45.1	88.4	16.7	45.9
3 ✓	45.4	51.9	56.9	31.6	54.8	37.4	41.2	87.7	14.5	38.0
4 ✓	55.2	64.0	67.1	39.2	68.9	41.0	44.2	88.4	17.8	47.2
5 ✓	55.6	65.7	68.9	38.4	70.8	40.9	44.1	88.8	17.4	46.1
6 ✓	54.4	64.9	63.9	38.8	69.4	35.6	43.7	88.5	11.6	41.3
7 ✓	<u>56.5</u>	65.8	<u>68.2</u>	40.1	<u>71.2</u>	<u>41.1</u>	44.2	<u>88.9</u>	<u>17.7</u>	48.2
8 ✓	56.9	65.8	70.4	<u>39.7</u>	71.5	41.3	<u>44.3</u>	89.5	<u>17.7</u>	48.2

Table 4: Finetuning evaluation of our disjoint trained models with varying pretraining datasets. We show results on VidSTG [83] (center) and VLN [60] (right). Each row is a model pretrained on the specified datasets and then finetuned on the downstream datasets. #0 is finetuned from a CLIP [48] checkpoint. Our disjoint-pretrained models (#4–#8) perform better than single-dataset pretrained ones (#0–#3), and yield the best CHOTA and AP_M on both VidSTG and VLN. The best entries are bolded, and the second-best underlined. Detailed caption metrics are in the supplement.

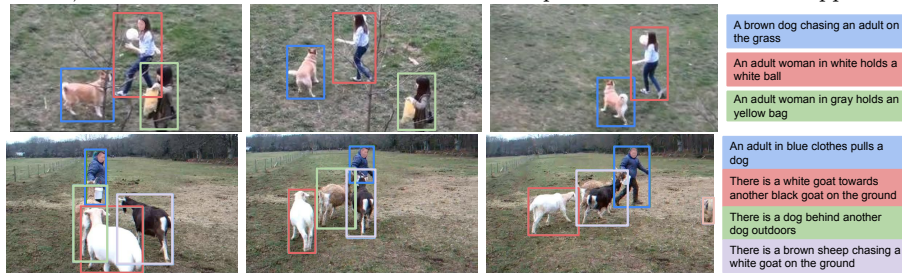


Fig. 4: Qualitative results on VidSTG. Our model captures motion (1st row) and handles crowded scenes (2nd row). However, it may misrecognize objects (2nd row, “dog” should be “goat”) and action boundaries (2nd row, “chasing” before it occurs).

Finetuning evaluation. We now finetune each of the pretrained models from Tab. 3 and show results in Tab. 4. We also include a baseline (#0) which initializes from only a CLIP-pretrained checkpoint [48], observing that this model performs poorly. If we pretrain on only a single dataset, we find that Visual Genome (VG) is the best, probably because it allows us to pretrain both the captioning- and object proposal modules (Fig. 3). Once again, we observe that different pretraining datasets are complementary, as adding either SMiT or COCO (#2 to #4, #2 to #5, #1 to #6) improves results further. Adding more pretraining datasets improves results further (#7), and we achieve the best results with our model pretrained on all pretraining datasets (#8), which outperforms the best single-dataset pretrained model by 2.0 CHOTA on VidSTG, and 0.7 CHOTA on VLN. The improvement over only a CLIP-pretrained checkpoint is even larger, by 9.1 CHOTA and 11.6 CHOTA on the two respective datasets. Qualitative visualizations are in Fig. 4 and the supplement.

4.6 State-of-the-art comparison on video grounding

As introduced in Sec. 3.5, models trained for Dense VOC can be directly used for sentence grounding, by finding the proposals with the maximum likelihood of

	Backbone	Recall&Prec. > 0.5
ReferFormer [60, 66]	ResNet50	48.3
GRiT [65]	ViT-B	62.1
Ours	ViT-B	65.1

Table 5: State-of-the-art comparison of spatial grounding on VLN Location-QA [60]. We report the official evaluation metric [60], which evaluates if both bounding box recall and precision are above 0.5. We compare to the VLN ReferFormer baseline [60, 66], GRiT [65], and our full model (#8 of Tab. 3).

	Finetuned	Zero-shot
STVGBert [56]	47.3	-
TubeDETR [72]	59.0	-
STCAT [31]	61.7	-
Ours	61.9	54.1

Table 6: State-of-the-art comparison of spatial grounding on the VidSTG test set. All models assume ground truth temporal localization is provided.

generating the query. We evaluate spatial grounding on the VLN Location-QA [60] and VidSTG [83] benchmarks respectively.

VLN Location-QA consists of questions starting with “Where is”, and requires the model to produce a bounding box at each frame in the video. The task is therefore effectively a sentence grounding problem, and indeed, the ReferFormer [66] baseline used by [60] performs sentence grounding after removing “Where is” from the question. We also remove this prefix before grounding following Sec. 3.5 for both our final model, and an additional GRiT baseline.

In this dataset, only one annotated frame (unknown at inference time) is evaluated, and this benchmark therefore effectively does not involve temporal localization. As the annotation of this dataset is based on mouse traces instead of bounding boxes, the evaluation metric considers bounding box coverage (recall) and precision (full details in [60]). As shown in Tab. 5, we improve substantially over ReferFormer and our GRiT [65] baseline.

VidSTG requires producing a sequence of bounding boxes for a given sentence query. The evaluation metric is the average of the Intersection over Union (IoU) at each frame, between the predicted and ground truth bounding boxes for the target object. We compare to other prior works on this dataset in Tab. 6, assuming that the input video is already trimmed temporally to the objects of interest. Our model achieves the best IoU, outperforming models designed specifically for grounding, thereby showing that our generative framework can be used effectively in the discriminative grounding task. In contrast to prior work, we also evaluate zero-shot without training on VidSTG, and still perform competitively. This result emphasizes the efficacy of our disjoint pretraining. We provide more results on VidSTG in the supplement.

5 Conclusion and Future Work

We proposed the new task of dense video object captioning. Although this task requires expensive annotations across space, time and language, we show that we can train a model on existing larger-scale datasets for disjoint subtasks. Moreover, our proposed end-to-end architecture is important for producing more accurate and coherent captions. Currently, our model produces a single caption for each trajectory, and in future work, we aim to caption potentially multiple action segments within one trajectory. We repurposed grounding datasets for our task, we aim to obtain a dataset with richer spatio-temporal captions in future.

Acknowledgments. We thank Shyamal Buch and Shen Yan for helpful feedback.

References

1. Alayrac, J.B., Donahue, J., Luc, P., Miech, A., Barr, I., Hasson, Y., Lenc, K., Mensch, A., Millican, K., Reynolds, M., et al.: Flamingo: a visual language model for few-shot learning. In: *NeurIPS (2022)* **1, 8**
2. Anderson, P., He, X., Buehler, C., Teney, D., Johnson, M., Gould, S., Zhang, L.: Bottom-up and top-down attention for image captioning and visual question answering. In: *CVPR (2018)* **3**
3. Antol, S., Agrawal, A., Lu, J., Mitchell, M., Batra, D., Zitnick, C.L., Parikh, D.: Vqa: Visual question answering. In: *ICCV (2015)* **1**
4. Arnab, A., Sun, C., Nagrani, A., Schmid, C.: Uncertainty-aware weakly supervised action detection from untrimmed videos. In: *ECCV (2020)* **8**
5. Banerjee, S., Lavie, A.: Meteor: An automatic metric for mt evaluation with improved correlation with human judgments. In: *ACL Workshops (2005)* **19**
6. Bellver, M., Ventura, C., Silberer, C., Kazakos, I., Torres, J., Giro-i Nieto, X.: Refvos: A closer look at referring expressions for video object segmentation. *arXiv:2010.00263 (2020)* **4**
7. Bewley, A., Ge, Z., Ott, L., Ramos, F., Upcroft, B.: Simple online and realtime tracking. In: *ICIP (2016)* **4**
8. Bilen, H., Vedaldi, A.: Weakly supervised deep detection networks. In: *CVPR (2016)* **8**
9. Bradbury, J., Frostig, R., Hawkins, P., Johnson, M.J., Leary, C., Maclaurin, D., Necula, G., Paszke, A., VanderPlas, J., Wanderman-Milne, S., Zhang, Q.: JAX: composable transformations of Python+NumPy programs (2018), <http://github.com/google/jax> **10**
10. Brown, T., Mann, B., Ryder, N., Subbiah, M., Kaplan, J.D., Dhariwal, P., Neelakantan, A., Shyam, P., Sastry, G., Askell, A., et al.: Language models are few-shot learners. In: *NeurIPS (2020)* **1**
11. Chen, X., Djolonga, J., Padlewski, P., Mustafa, B., Changpinyo, S., Wu, J., Ruiz, C.R., Goodman, S., Wang, X., Tay, Y., et al.: Pali-x: On scaling up a multilingual vision and language model. In: *arXiv preprint arXiv:2305.18565 (2023)* **1**
12. Chen, X., Wang, X., Changpinyo, S., Piergiovanni, A., Padlewski, P., Salz, D., Goodman, S., Grycner, A., Mustafa, B., Beyler, L., et al.: Pali: A jointly-scaled multilingual language-image model. In: *ICLR (2023)* **8**
13. Chen, X., Fang, H., Lin, T.Y., Vedantam, R., Gupta, S., Dollár, P., Zitnick, C.L.: Microsoft coco captions: Data collection and evaluation server. *arXiv:1504.00325 (2015)* **1, 2, 3, 10**
14. Cheng, B., Misra, I., Schwing, A.G., Kirillov, A., Girdhar, R.: Masked-attention mask transformer for universal image segmentation. In: *CVPR (2022)* **4**
15. Cheng, H.K., Oh, S.W., Price, B., Lee, J.Y., Schwing, A.: Putting the object back into video object segmentation. In: *CVPR (2024)* **4**
16. Cheng, H.K., Schwing, A.G.: XMem: Long-term video object segmentation with an atkinson-shiffrin memory model. In: *ECCV (2022)* **4**
17. Dave, A., Khurana, T., Tokmakov, P., Schmid, C., Ramanan, D.: Tao: A large-scale benchmark for tracking any object. In: *ECCV (2020)* **2, 8**
18. Dehghani, M., Gritsenko, A., Arnab, A., Minderer, M., Tay, Y.: Scenic: A jax library for computer vision research and beyond. In: *CVPR (2022)* **10**
19. Dendorfer, P., Osep, A., Milan, A., Schindler, K., Cremers, D., Reid, I., Roth, S., Leal-Taixé, L.: Motchallenge: A benchmark for single-camera multiple target tracking. *IJCV (2021)* **2, 4, 8**

20. Desai, K., Johnson, J.: Virtex: Learning visual representations from textual annotations. In: CVPR (2021) [3](#)
21. Devlin, J., Chang, M.W., Lee, K., Toutanova, K.: Bert: Pre-training of deep bidirectional transformers for language understanding. In: NAACL (2019) [3](#)
22. Dosovitskiy, A., Beyer, L., Kolesnikov, A., Weissenborn, D., Zhai, X., Unterthiner, T., Dehghani, M., Minderer, M., Heigold, G., Gelly, S., et al.: An image is worth 16x16 words: Transformers for image recognition at scale. In: ICLR (2021) [3](#), [10](#), [20](#)
23. Du, Y., Guo, W., Xiao, Y., Lepetit, V.: 1st place solution for the uvo challenge on video-based open-world segmentation 2021. arXiv:2110.11661 (2021) [4](#)
24. Everingham, M., Eslami, S.A., Van Gool, L., Williams, C.K., Winn, J., Zisserman, A.: The pascal visual object classes challenge: A retrospective. IJCV (2015) [2](#), [19](#)
25. Geiger, A., Lenz, P., Urtasun, R.: Are we ready for autonomous driving? the kitti vision benchmark suite. In: CVPR (2012) [4](#), [8](#)
26. Graves, A.: Generating sequences with recurrent neural networks. arXiv:1308.0850 (2013) [5](#)
27. He, K., Gkioxari, G., Dollár, P., Girshick, R.: Mask r-cnn. In: ICCV (2017) [4](#), [5](#)
28. Hendricks, L.A., Burns, K., Saenko, K., Darrell, T., Rohrbach, A.: Women also snowboard: Overcoming bias in captioning models. In: ECCV (2018) [24](#)
29. Hochreiter, S., Schmidhuber, J.: Long short-term memory. Neural computation (1997) [4](#)
30. Jiang, H., Misra, I., Rohrbach, M., Learned-Miller, E., Chen, X.: In defense of grid features for visual question answering. In: CVPR (2020) [3](#)
31. Jin, Y., Yuan, Z., Mu, Y., et al.: Embracing consistency: A one-stage approach for spatio-temporal video grounding. In: NeurIPS (2022) [4](#), [14](#), [23](#)
32. Johnson, J., Karpathy, A., Fei-Fei, L.: Densecap: Fully convolutional localization networks for dense captioning. In: CVPR (2016) [3](#), [4](#)
33. Krishna, R., Hata, K., Ren, F., Fei-Fei, L., Carlos Niebles, J.: Dense-captioning events in videos. In: ICCV (2017) [4](#)
34. Krishna, R., Zhu, Y., Groth, O., Johnson, J., Hata, K., Kravitz, J., Chen, S., Kalantidis, Y., Li, L.J., Shamma, D.A., et al.: Visual genome: Connecting language and vision using crowdsourced dense image annotations. IJCV (2017) [1](#), [3](#), [8](#), [10](#), [19](#)
35. Li, J., Li, D., Savarese, S., Hoi, S.: Blip-2: Bootstrapping language-image pre-training with frozen image encoders and large language models. In: ICML (2023) [1](#), [3](#)
36. Li, X., Zhang, W., Pang, J., Chen, K., Cheng, G., Tong, Y., Loy, C.C.: Video k-net: A simple, strong, and unified baseline for video segmentation. In: CVPR (2022) [4](#)
37. Li, X., Jiang, S., Han, J.: Learning object context for dense captioning. In: AAAI (2019) [3](#)
38. Li, X., Yin, X., Li, C., Zhang, P., Hu, X., Zhang, L., Wang, L., Hu, H., Dong, L., Wei, F., et al.: Oscar: Object-semantics aligned pre-training for vision-language tasks. In: ECCV (2020) [3](#)
39. Li, Y., Mao, H., Girshick, R., He, K.: Exploring plain vision transformer backbones for object detection. In: ECCV (2022) [10](#), [20](#)
40. Lin, T.Y., Goyal, P., Girshick, R., He, K., Dollár, P.: Focal loss for dense object detection. In: ICCV (2017) [5](#), [21](#)
41. Lin, T.Y., Maire, M., Belongie, S., Hays, J., Perona, P., Ramanan, D., Dollár, P., Zitnick, C.L.: Microsoft coco: Common objects in context. In: ECCV (2014) [2](#), [3](#), [8](#), [19](#)
42. Liu, H., Li, C., Wu, Q., Lee, Y.J.: Visual instruction tuning. In: NeurIPS (2023) [1](#)

43. Long, Y., Wen, Y., Han, J., Xu, H., Ren, P., Zhang, W., Zhao, S., Liang, X.: Capdet: Unifying dense captioning and open-world detection pretraining. In: CVPR (2023) [1](#)
44. Luiten, J., Osep, A., Dendorfer, P., Torr, P., Geiger, A., Leal-Taixé, L., Leibe, B.: Hota: A higher order metric for evaluating multi-object tracking. IJCV (2021) [2](#), [9](#), [10](#)
45. Monfort, M., Jin, S., Liu, A., Harwath, D., Feris, R., Glass, J., Oliva, A.: Spoken moments: Learning joint audio-visual representations from video descriptions. In: CVPR (2021) [1](#), [2](#), [3](#), [8](#)
46. Ouyang, L., Wu, J., Jiang, X., Almeida, D., Wainwright, C., Mishkin, P., Zhang, C., Agarwal, S., Slama, K., Ray, A., et al.: Training language models to follow instructions with human feedback. In: NeurIPS (2022) [1](#)
47. Perazzi, F., Pont-Tuset, J., McWilliams, B., Van Gool, L., Gross, M., Sorkine-Hornung, A.: A benchmark dataset and evaluation methodology for video object segmentation. In: CVPR (2016) [4](#)
48. Radford, A., Kim, J.W., Hallacy, C., Ramesh, A., Goh, G., Agarwal, S., Sastry, G., Askell, A., Mishkin, P., Clark, J., et al.: Learning transferable visual models from natural language supervision. In: ICML (2021) [1](#), [3](#), [10](#), [13](#), [20](#)
49. Raffel, C., Shazeer, N., Roberts, A., Lee, K., Narang, S., Matena, M., Zhou, Y., Li, W., Liu, P.J.: Exploring the limits of transfer learning with a unified text-to-text transformer. JMLR (2020) [1](#)
50. Redmon, J., Divvala, S., Girshick, R., Farhadi, A.: You only look once: Unified, real-time object detection. In: CVPR (2016) [4](#)
51. Ren, S., He, K., Girshick, R., Sun, J.: Faster r-cnn: Towards real-time object detection with region proposal networks. In: NeurIPS (2015) [5](#)
52. Rennie, S.J., Marcheret, E., Mroueh, Y., Ross, J., Goel, V.: Self-critical sequence training for image captioning. In: CVPR (2017) [3](#)
53. Shang, X., Di, D., Xiao, J., Cao, Y., Yang, X., Chua, T.S.: Annotating objects and relations in user-generated videos. In: ICMR (2019) [9](#)
54. Shao, Z., Han, J., Marnerides, D., Debattista, K.: Region-object relation-aware dense captioning via transformer. IEEE Transactions on Neural Networks and Learning Systems (2022) [3](#)
55. Sharma, P., Ding, N., Goodman, S., Soricut, R.: Conceptual captions: A cleaned, hypernymed, image alt-text dataset for automatic image captioning. In: ACL (2018) [3](#)
56. Su, R., Yu, Q., Xu, D.: Stvgbert: A visual-linguistic transformer based framework for spatio-temporal video grounding. In: ICCV (2021) [4](#), [14](#), [23](#)
57. Team, G., Anil, R., Borgeaud, S., Wu, Y., Alayrac, J.B., Yu, J., Soricut, R., Schalkwyk, J., Dai, A.M., Hauth, A., et al.: Gemini: a family of highly capable multimodal models. arXiv:2312.11805 (2023) [1](#)
58. Union, G.I.O.: A metric and a loss for bounding box regression. In: CVPR (2019) [21](#)
59. Vaswani, A., Shazeer, N., Parmar, N., Uszkoreit, J., Jones, L., Gomez, A.N., Kaiser, Ł., Polosukhin, I.: Attention is all you need. In: NeurIPS (2017) [3](#), [4](#), [5](#)
60. Voigtlaender, P., Changpinyo, S., Pont-Tuset, J., Soricut, R., Ferrari, V.: Connecting vision and language with video localized narratives. In: CVPR (2023) [2](#), [4](#), [8](#), [9](#), [12](#), [13](#), [14](#), [19](#), [20](#)
61. Wang, J., Yang, Z., Hu, X., Li, L., Lin, K., Gan, Z., Liu, Z., Liu, C., Wang, L.: Git: A generative image-to-text transformer for vision and language. TMLR (2022) [3](#), [4](#), [5](#), [7](#), [20](#), [21](#)

62. Wang, T., Zhang, R., Lu, Z., Zheng, F., Cheng, R., Luo, P.: End-to-end dense video captioning with parallel decoding. In: ICCV (2021) [4](#)
63. Wang, W., Feiszli, M., Wang, H., Tran, D.: Unidentified video objects: A benchmark for dense, open-world segmentation. In: ICCV (2021) [8](#), [9](#), [22](#)
64. Wang, Y., Xu, Z., Wang, X., Shen, C., Cheng, B., Shen, H., Xia, H.: End-to-end video instance segmentation with transformers. In: CVPR (2021) [4](#)
65. Wu, J., Wang, J., Yang, Z., Gan, Z., Liu, Z., Yuan, J., Wang, L.: Grit: A generative region-to-text transformer for object understanding. arXiv:2212.00280 (2022) [1](#), [3](#), [4](#), [5](#), [10](#), [11](#), [14](#), [20](#)
66. Wu, J., Jiang, Y., Sun, P., Yuan, Z., Luo, P.: Language as queries for referring video object segmentation. In: CVPR (2022) [4](#), [14](#)
67. Wu, Y., Kirillov, A., Massa, F., Lo, W.Y., Girshick, R.: Detectron2. <https://github.com/facebookresearch/detectron2> (2019) [11](#)
68. Xu, J., Mei, T., Yao, T., Rui, Y.: Msr-vtt: A large video description dataset for bridging video and language. In: CVPR (2016) [3](#)
69. Xu, K., Ba, J., Kiros, R., Cho, K., Courville, A., Salakhudinov, R., Zemel, R., Bengio, Y.: Show, attend and tell: Neural image caption generation with visual attention. In: ICML (2015) [3](#)
70. Xu, N., Yang, L., Fan, Y., Yang, J., Yue, D., Liang, Y., Price, B., Cohen, S., Huang, T.: Youtube-vos: Sequence-to-sequence video object segmentation. In: ECCV (2018) [4](#)
71. Yan, S., Zhu, T., Wang, Z., Cao, Y., Zhang, M., Ghosh, S., Wu, Y., Yu, J.: Video-text modeling with zero-shot transfer from contrastive captioners. arXiv:2212.04979 (2022) [3](#)
72. Yang, A., Miech, A., Sivic, J., Laptev, I., Schmid, C.: Tubedetr: Spatio-temporal video grounding with transformers. In: CVPR (2022) [4](#), [14](#), [23](#)
73. Yang, A., Nagrani, A., Seo, P.H., Miech, A., Pont-Tuset, J., Laptev, I., Sivic, J., Schmid, C.: Vid2seq: Large-scale pretraining of a visual language model for dense video captioning. In: CVPR (2023) [4](#)
74. Yang, L., Fan, Y., Xu, N.: Video instance segmentation. In: ICCV (2019) [4](#), [8](#)
75. Yang, Z., Wang, X., Miao, J., Wei, Y., Wang, W., Yang, Y.: Scalable video object segmentation with identification mechanism. arXiv preprint arXiv:2203.11442 (2023) [4](#)
76. Yang, Z., Wei, Y., Yang, Y.: Associating objects with transformers for video object segmentation. In: NeurIPS (2021) [4](#)
77. Yang, Z., Yang, Y.: Decoupling features in hierarchical propagation for video object segmentation. In: NeurIPS (2022) [4](#)
78. Yu, J., Wang, Z., Vasudevan, V., Yeung, L., Seyedhosseini, M., Wu, Y.: Coca: Contrastive captioners are image-text foundation models. TMLR (2022) [3](#)
79. Yu, L., Poirson, P., Yang, S., Berg, A.C., Berg, T.L.: Modeling context in referring expressions. In: ECCV (2016) [4](#)
80. Zhang, P., Li, X., Hu, X., Yang, J., Zhang, L., Wang, L., Choi, Y., Gao, J.: Vinvl: Revisiting visual representations in vision-language models. In: CVPR (2021) [3](#)
81. Zhang, Y., Sun, P., Jiang, Y., Yu, D., Weng, F., Yuan, Z., Luo, P., Liu, W., Wang, X.: Bytetrack: Multi-object tracking by associating every detection box. In: ECCV (2022) [11](#)
82. Zhang, Y., Wang, C., Wang, X., Zeng, W., Liu, W.: Fairmot: On the fairness of detection and re-identification in multiple object tracking. IJCV (2021) [4](#), [7](#), [8](#), [11](#)
83. Zhang, Z., Zhao, Z., Zhao, Y., Wang, Q., Liu, H., Gao, L.: Where does it exist: Spatio-temporal video grounding for multi-form sentences. In: CVPR (2020) [2](#), [4](#), [8](#), [9](#), [12](#), [13](#), [14](#), [19](#), [20](#), [22](#), [23](#)

84. Zhao, D., Wang, A., Russakovsky, O.: Understanding and evaluating racial biases in image captioning. In: ICCV (2021) 24
85. Zhou, L., Xu, C., Corso, J.: Towards automatic learning of procedures from web instructional videos. In: AAAI (2018) 3, 4
86. Zhou, X., Girdhar, R., Joulin, A., Krähenbühl, P., Misra, I.: Detecting twenty-thousand classes using image-level supervision. In: ECCV (2022) 7, 8
87. Zhou, X., Koltun, V., Krähenbühl, P.: Tracking objects as points. In: ECCV (2020) 7, 8
88. Zhou, X., Wang, D., Krähenbühl, P.: Objects as points. arXiv:1904.07850 (2019) 5, 10, 20
89. Zhou, X., Yin, T., Koltun, V., Krähenbühl, P.: Global tracking transformers. In: CVPR (2022) 4, 6, 8

We present further additional experimental details (App. A), additional experimental analysis (App. B), and broader impact and potential negative impact (App. C).

A Additional Experimental and Implementation Details

A.1 AP_M implementation details

mAP-METEOR is the official evaluation metric used in Visual Genome [34] dataset for dense image object captioning. This metric evaluates predictions in each frame separately, without evaluating the tracking output.

mAP-METEOR is based on the Average Precision used in object detection [24, 41], but includes a caption similarity criteria for determining true positives: *i.e.* a prediction is a true positive if the Intersection over Union (IoU) with the ground truth bounding box is above a threshold, *and* if the METEOR score [5] is above another threshold. We follow the same implementation and thresholds as the Visual Genome dataset*. *i.e.* IoU thresholds of (0.3, 0.4, 0.5, 0.6, 0.7) and METEOR thresholds of (0.0, 0.05, 0.1, 0.15, 0.2).

In our case, some objects in the datasets [60, 83] only have bounding box annotations and no caption annotations (Sec. 4.1.1). For these objects without caption annotations, we allow any caption prediction (and therefore ignore it) by setting its METEOR score to the maximum of 1. For brevity, we abbreviated this metric as AP_M in the main paper.

A.2 CHOTA Details and Evaluation code

We attach our CHOTA evaluation code as `chota.py`. This evaluation code is based on the official HOTA implementation*. The original code is under an MIT license.

* https://github.com/jcjohnson/densecap/blob/master/eval/eval_utils.lua

* <https://github.com/JonathonLuiten/TrackEval>

A.3 Full training details

As mentioned in Sec. 4.1.3, our model is based on GRiT [65]. The original GRiT code* is released under an MIT license. Following GRiT, we use a ViTDet-Base [22, 39] backbone, a CenterNet [88] region proposal network and RoI Head, and a randomly-initialized text decoder following that of GIT [61]. The text decoder consists of 6 self-attention layers with casual feature masks [61]. All model architecture parameters follow the defaults from GRiT [65].

The original GRiT uses an MAE pretrained checkpoint, while in our case we found a CLIP pretrained checkpoint [48] performs better on our task. To fit more frames into memory for both training and evaluation, we use a 384×384 input size instead of the original 1024×1024 . This choice moderately decreases dense image captioning performance on Visual Genome (from 17.3 AP_M to 15.7 AP_M).

During disjoint multi-dataset pretraining, we sample batches from different datasets in an even ratio (1 : 1 : 1 : 1). For image datasets, a batch is composed of different images; for video datasets, we put the time dimension in batches and always guarantee images in the same mini-batch are from the same video. We use a local batch size of either 1 video (consisting of 8 sampled frames), or 8 images. As we use 32 TPUs, this means that our global batch size is either 32 videos or 256 images. We use the AdamW optimizer with a learning rate of 2×10^{-4} , weight decay of 0.05, and a layerwise learning rate decay of 0.7 [39, 65]. We train for 22.5×10^3 iterations per dataset, decreasing the learning rate by a factor of 10 after 90% and 97.5% of the training schedule [65]. For pretraining on all the 4 datasets in Sec. 3.4, this corresponds to a total of 90×10^3 iterations, which took approximately 20 hours on 32, 16GB TPUs cores.

For VidSTG [83] finetuning, we sample 16 frames in training, and run on all 200 frames in testing. For VLN [60] finetuning, we use the 3 annotated frames in both training and evaluation. For finetuning experiments on both datasets, we use a video batch size 16 and train for 11.25×10^3 iterations, with a learning rate of 10^{-5} , weight decay of 0.05, and layerwise-learning decay of 0.7 [39]. The finetuning took approximately 6 hours on 16, 16GB TPUs for VidSTG, and about 2 hours on 16, 16GB TPUs for VLN. Inference on VidSTG requires 32GB of TPU memory to fit 200 frames.

Training losses. Training our model involves a detection loss L_{object} , a tracking loss L_{assoc} , and a captioning loss $L_{caption}$, that is

$$L = L_{object} + L_{assoc} + L_{caption}. \quad (3)$$

For completeness, we detail these three terms next:

The detection loss [88] involves a center heatmap loss, a bounding box regression loss, and a classification and bounding box refinement loss in the RoI head:

$$L_{object} = L_{heatmap} + L_{reg} + L_{roi-cls} + L_{roi-reg}. \quad (4)$$

* <https://github.com/JialianW/GRiT>

The heatmap loss is defined on the predicted heatmap $Y \in \mathbb{R}^{H \times W}$ and the ground truth heatmap $\bar{Y} \in \mathbb{R}^{H \times W}$:

$$L_{heatmap}(Y, \bar{Y}) = \frac{1}{n} \sum_{ij} \begin{cases} (1 - Y_{ij})^\alpha \log(Y_{ij}) & \text{if } \bar{Y}_{ij} = 1 \\ (1 - \bar{Y}_{ij})^\beta (Y_{ij})^\alpha \log(1 - Y_{ij}) & \text{otherwise,} \end{cases} \quad (5)$$

where n is the number of objects in the image, $\alpha = 2$ and $\beta = 4$ are the focal loss weights [40].

L_{reg} is a gIoU loss [58]:

$$L_{reg}(B, \bar{B}) = \frac{1}{n} \sum_i (\text{IoU}(B_i, \bar{B}_i) - \frac{|C_i \setminus (B_i \cup \bar{B}_i)|}{|C_i|}), \quad (6)$$

where B and \bar{B} are the predicted and the ground truth bounding boxes of the n annotated objects, C_i is the enclosing convex hull of B_i and \bar{B}_i , and $|\cdot|$ computes the area.

$L_{roi-cls}$ is a softmax classification loss on each RoI box, defined on the predicted class logits $\mathbf{c} \in \mathbb{R}^2$ and the ground truth label $\bar{c} \in \{0, 1\}$. Here we only have foreground or background classification.

$$L_{roi-cls}(\mathbf{c}, \bar{c}) = -\log \text{softmax}(\mathbf{c})_{\bar{c}} \quad (7)$$

$L_{roi-reg}$ is an L1 loss between the predicted boxes B and the ground truth boxes \bar{B} ,

$$L_{roi-reg}(B, \bar{B}) = |B - \bar{B}|. \quad (8)$$

The tracking loss is a per-element binary cross-entropy loss between the predicted association matrix A and the ground truth binary matrix \bar{A} :

$$L_{assoc} = -\frac{1}{M} \sum_{ij} (\hat{A}_{ij} \log A_{ij} + (1 - \hat{A}_{ij}) \log (1 - A_{ij})). \quad (9)$$

The captioning loss is a softmax on each predicted word over the entire vocabulary, with a label smoothing co-efficient of 0.1 following GIT [61].

$$L_{caption} = \frac{1}{L} \sum_{i=1}^L \text{CE}(\text{Decode}(f, \bar{y}_{1:i-1}), \bar{y}_i), \quad (10)$$

where \bar{y} is the ground truth caption, L is the ground-truth sentence length, and f is the object feature.

B Additional Experimental Analysis

B.1 Ablation of hard tracking sampling.

We analyze the effect of the number of sampled frames, m , in hard-aggregation (Sec. 3.3) in Tab. 7. With hard-aggregation, the captioning accuracy benefits from a larger number of frames m , thanks to longer input-sequence length. However, this also costs more TPU memory in both training and testing. We use $m = 6$ in our ablation experiments (Tab. 2) as it achieves the best accuracy. It also follows the default number of frames used in the GIT [61] video captioning model.

m	CHOTA(\uparrow)	DetA(\uparrow)	AssA(\uparrow)	CapA(\uparrow)	AP $_M$ (\uparrow)
1	53.6	64.3	66.3	36.1	68.7
2	54.1	64.3	66.2	37.3	68.7
4	54.4	64.3	65.7	37.8	68.7
6	54.9	64.2	65.9	39.1	69.1
8	54.6	64.3	66.1	38.4	69.1

Table 7: Hyper-parameter sweep for number of sampled frames, m , for hard-tracking. We show results on VidSTG [83] validation set. The models are based on #2 of Tab. 4 on VidSTG. Results with hard-feature aggregation get improved with more sampled frames and get saturated with 6 frames.

Tracking dataset	CHOTA	DetA	AssA	CapA	AP $_M$
<i>Zero-shot</i>					
UVO		24.8	41.2	52.1	7.1 33.8
Aug-COCO	31.1	51.4	59.6	9.8	39.5
<i>Finetuning</i>					
UVO		50.9	65.2	53.4	37.9 70.4
Aug-COCO	56.9	65.8	70.4	39.7	71.5

Table 8: Results using UVO [63] as the tracking dataset. We show both zero-shot results (top) and finetuning results (bottom) on VidSTG datasets. For reference, we also include our results of using Aug-COCO (#8 of Tab. 3 and Tab. 4). Aug-COCO performs better in both settings, motivating our choice in the main paper.

B.2 Using the UVO dataset for disjoint pretraining

For the disjoint pretraining of our model (Sec. 3.4), we used Augmented COCO as our tracking dataset. Another alternative would have been to use UVO [63], which contains real-world videos, but is relatively small at only 5000 videos.

Table 8 compares Aug-COCO and UVO under the setting of Tab. 3 and Tab. 4 #8, both using a default multi-dataset sampling ratio 1 : 1 : 1 : 1. We observe that disjoint pretraining with Aug-COCO consistently performs better than UVO in both zero-shot and finetuning scenarios, thus motivating our choice to use Aug-COCO for our experiments in the main paper.

B.3 Detailed captioning results

The Captioning Accuracy (CapA) component of our CHOTA metric is the average of the CIDEr, METEOR and SPICE metrics. For completeness, we report each of these captioning metrics individually in Tabs. 9 and 10, for zero-shot and full-finetuning evaluation, respectively.

B.4 VidSTG spatio-temporal grounding evaluation

Table 6 of the main paper compared to prior methods on the spatial-video grounding task on VidSTG (where the input videos were assumed to already be

#	COCO	VG	SMiT	Aug-COCO	VidSTG			VLN				
					CapA	CIDEr	METEOR	SPICE	CapA	CIDEr	METEOR	SPICE
1	✓				-	-	-	-	-	-	-	
2		✓			7.8	4.2	7.1	12.1	7.4	2.7	7.4	12.1
3			✓		-	-	-	-	-	-	-	
4		✓	✓		8.5	4.4	7.7	13.4	8.5	3.1	8.7	13.8
5	✓	✓			8.1	4.0	7.2	13.0	7.8	3.1	7.8	12.4
6	✓		✓		4.9	3.3	7.2	4.2	7.5	3.7	9.4	9.6
7	✓	✓	✓		9.1	5.2	8.3	13.7	9.0	3.9	9.2	13.9
8	✓	✓	✓	✓	9.8	7.0	9.1	13.3	9.7	4.6	9.9	14.6

Table 9: Detailed captioning metrics of our *zero-shot evaluation* (Tab. 3). We show the individual captioning metrics CIDEr, METEOR, and SPICE for each row on both datasets.

#	COCO	VG	SMiT	Aug-COCO	VidSTG			VLN				
					CapA	CIDEr	METEOR	SPICE	CapA	CIDEr	METEOR	SPICE
0					35.8	43.2	29.0	35.0	8.7	3.9	14.8	7.3
1	✓				34.8	41.7	27.5	35.5	8.2	6.7	14.0	3.9
2		✓			39.1	49.4	30.3	37.6	16.7	13.9	20.1	16.1
3			✓		31.6	33.8	27.2	33.6	14.5	9.6	19.6	14.2
4		✓	✓		39.2	49.9	30.3	37.5	17.8	13.9	21.4	17.9
5	✓	✓			38.4	48.3	30.0	36.9	17.4	15.1	20.5	16.5
6	✓		✓		38.8	49.6	29.9	37.1	11.6	8.2	17.3	9.5
7	✓	✓	✓		40.1	51.5	30.8	38.1	17.7	14.6	21.5	17.1
8	✓	✓	✓	✓	39.7	51.0	30.6	37.7	17.7	14.3	21.5	17.5

Table 10: Detailed captioning metrics of our *finetuning evaluation* (Tab. 4). We show the individual captioning metrics CIDEr, METEOR, and SPICE for each row on both datasets.

	Validation set			Test set		
	sIoU	tIoU	vIoU	sIoU	tIoU	vIoU
STGRN [83]	-	-	-	38.0	48.5	19.8
STVGBert [56]	-	-	-	47.3	-	24.0
TubeDETR [72]	56.4	47.2	28.7	59.0	48.1	30.4
STCAT [31]	-	-	-	61.7	50.8	33.1
Ours (zero-shot)	51.8	40.0	22.0	54.1	40.2	22.5
Ours	58.7	41.8	25.9	61.9	41.1	26.3

Table 11: State-of-the-art comparison of spatial-temporal grounding on VidSTG. “-” means the numbers are not reported in the paper. Our model performs competitively at this task, although it was not actually designed for it. As our model generates object trajectories without conditioning on the input query, it struggles at temporal localization, denoted by the tIoU. The spatial localization performance, denoted by the sIoU, outperforms dedicated methods for this task.

temporally trimmed). In Tab. 11, we report results for spatial-, temporal- and spatio-temporal grounding by reporting the Spatial IoU (sIoU), Temporal IoU (tIoU) and Video IoU (vIoU) respectively.

The sIoU assumes the video is already temporally trimmed before evaluation, thus evaluating spatial localization. Similarly, the tIoU assumes that the video is

already cropped spatially around the object of interest, and only the temporal extent of the query sentence needs to be determined, thereby evaluating temporal localization. The vIoU evaluates both spatial and temporal localization.

Our model was designed for the Dense VOC task, and not grounding, and we were able to perform grounding by selecting the bounding boxes with the highest likelihood of generating the target sentence (Sec. 3.5). As shown in Tab. 11, this approach works well for spatial-grounding, outperforming prior works in terms of the sIoU. However, as our model first generates object trajectories, without taking the input query into account, it struggles more at temporal localization. Nevertheless, it still achieves competitive results compared to prior works for both the tIoU and vIoU, although our model was not designed specifically for this task like the other methods in Tab. 11 which include explicit temporal localization modules within the network.

C Broader impact and potential negative impact

Our work presents a new task and model for dense video object captioning. This task represents a general technology with a wide range of potential applications. Whilst we are unaware of all potential applications of such models, it is important to be cognizant that each application has its own merits and societal implications depending on the intentions of the individuals building and using the system. For example, we believe that the Dense VOC models can be used as part of systems to improve video search and retrieval, though they could also be used in video surveillance systems too. Additionally, we note that training datasets, especially for captioning [28, 84], can contain biases that may render models trained on them unsuitable for deployment.